Bruton tyrosine kinase covalent inhibition shapes the immune microenvironment in chronic lymphocytic leukemia

Daniel Medina-Gil,[1,2] Laura Palomo,[1,2] Víctor Navarro,[3] Gonzalo Lázaro,[4] Beatriz Martín-Mur,[5] Cristina Hernández,[1,2] Oriol Castells,[1,2] Belén Sánchez,[1,2] Pau Marc Muñoz-Torres,[6] Carlota Pagès,[1,2] Gemma Pujadas,[1,2] Anna Esteve-Codina,[5] Alba Cabirta,[2,7] Christelle Ferrà,[8] Miguel Alcoceba,[9] Maria José Terol,[10] Rafael Andreu,[11] Mercè Martí,[4] Pau Abrisqueta,[2,7] Francesc Bosch[2,7] and Marta Crespo[1,2] on behalf of the Spanish Group of Chronic Lymphocytic Leukemia (GELLC)

[1]Experimental Hematology, Vall d'Hebron Institute of Oncology (VHIO), Vall d'Hebron Barcelona Hospital Campus, Barcelona; [2]Department of Medicine, Universitat Autònoma de Barcelona, Bellaterra; [3]Oncology Data Science (ODysSey) Group, Vall d'Hebron Institute of Oncology (VHIO), Vall d'Hebron Barcelona Hospital Campus, Barcelona; [4]Immunology Unit, Department of Cell Biology, Physiology and Immunology, Institut de Biotecnologia i Biomedicina (IBB), Universitat Autònoma de Barcelona, Bellaterra; [5]CNAG-CRG, Center for Genomic Regulation, Barcelona Institute of Science and Technology, Barcelona; [6]Bioinformatic Unit, Vall d'Hebron Institute of Oncology (VHIO), Vall d'Hebron Barcelona Hospital Campus, Barcelona; [7]Servei d'Hematologia, Vall d'Hebron Hospital Universitari, Experimental Hematology, Vall d'Hebron Institute of Oncology (VHIO), Vall d'Hebron Barcelona Hospital Campus, Barcelona; [8]Department of Hematology, Institut Català d'Oncologia - Hospital Germans Trias i Pujol, Josep Carreras Research Institute, Badalona; [9]Department of Hematology, Cancer Research Institute of Salamanca, University Hospital of Salamanca, Salamanca; [10]Department of Hematology, Hospital Clínico Universitario de Valencia, Valencia and [11]Department of Hematology, Hospital Universitario Politécnico "La Fe", Valencia, Spain

Correspondence: M. Crespo
macrespo@vhio.net

F. Bosch
fbosch@vhio.net

Received: September 17, 2024.
Accepted: February 28, 2025.
Early view: March 13, 2025.

https://doi.org/10.3324/haematol.2024.286663

EXTENDED METHODS

Flow cytometry

Cryopreserved PBMCs were thawed at 37ºC in RPMI 1640 media. Cells were stained at $10x10^6$ cells/mL in a final volume of 100μl of PBS + BSA 0.5% + 0.1% sodium azide at room temperature for 15 minutes. Fluorochrome-conjugated antibody information is listed in **Table S2**. Samples were acquired by Navios EX Flow Cytometer (Beckman Coulter) and data was analyzed using FlowJo Software (BD Biosciences). Blood counts were used to calculate absolute numbers of lymphocyte subpopulations.

T cell proliferation and cytokine production assays

PBMCs from CLL patients were initially labeled with carboxylfluorescein succinimidyl ester (CFSE) (Thermo Fisher Scientific) (5μM). Cells were stimulated with Dynabeads Human T-Activator CD3/CD28 (Gibco) in a ratio of 1:10 T cells for 3 days at $5x10^6$ cells/mL in 200μL of IMDM GlutaMAX media (Gibco) complemented with 10% of decomplemented human serum and 1x antibiotic/antimycotic (Gibco) at 37ºC 5% CO_2. Cell supernatants were collected and frozen at -20ºC. Levels of IL-2, IL-4, IL-6, IL-10, IL17A, IFNγ, TNFα, sFas, sFasL, granzyme A, granzyme B, perforin, and granulysin were measured with the LEGENDplex Human CD8/NK Panel (13-plex) (Biolegend) from cell culture supernatants following manufacturer's protocol. Stimulated cells were stained with CD3-PC7 (BD Biosciences) (1:50), CD4-PC5.5 (Beckman Coulter) (1:50) and CD8-APC-Cy7 (Biolegend) (1:50) and LIVE/DEAD Fixable Violet Dead Cell stain (Thermo Fisher Scientific), and CFSE intensity was analyzed. Proliferation and cytokine production levels of PBMCs from 6 age-matched HD cultured at $1x10^6$ cells/mL were also measured as a reference control group.

For intracellular staining, two million PBMCs from CLL patients and age-matched HD were stimulated with PMA (50ng/mL) and ionomycin (1μg/mL) (Biolegend) with Golgi inhibition with 5μg/mL of brefeldin A (BFA) (Biolegend) for 4h at 37ºC 5% CO_2 in 1mL of complete IMDM GlutaMAX media (Gibco). Extracellular staining included CD19-PE (BD Biosciences) (1:50), CD3-ECD (Beckman Coulter) (1:50), CD4-PC5.5 (Beckman Coulter) (1:50), CD107a-APC (Biolegend) (1:100) and CD8-APC-Cy7 (Biolegend) (1:50). Cells were also stained with LIVE/DEAD Fixable Violet Dead Cell stain (Thermo Fisher Scientific) (1:1000) to discriminate dead cells. For intracellular staining, we followed Invitrogen eBioscience FOXP3/Transcription Factor Staining Buffer Set protocol (Thermo Fisher Scientific). Intracellular staining included Granzyme B-FITC (Biolegend) (1:50) and IFNγ-PC7 (Thermo Fisher Scientific) (1:50).

Chemokine determination

Chemokine determination in plasma was performed by using a custom ProcartaPlex Immunoassay kit of Luminex (Thermo Fisher Scientific) including CCL2, CCL3, CCL4, CXCL10, CXCL13, CCL19, CXCL12, CXCL1 and IL-8. CXCL1 and IL-8 levels were not detected. Duplicates and triplicates for each sample were included. Bead acquisition was performed by MAPGIX (Thermo Fisher Scientific). Data analysis was performed in ProcartaPlex Analysis App (Thermo Fisher Scientific). All the samples had a coefficient of variation <30% between replicates. The lower limit of quantification value was assigned in plasma samples at 6 months of ibrutinib timepoint with undetectable levels.

Migration assay

An initial B cell enrichment was performed by using EasySep Human B Cell Enrichment w/o CD43 Depletion kit (Stem cell). $2x10^6$ cells in 100μL were added in the top chamber of 24-well polystyrene inserts of 5.0μm pore size (Corning). Cells were allowed to migrate towards CXCL12 (200ng/ml) (Peprotech) in RPMI media + BSA 0.5% (Sigma-Aldrich) for 4 hours in triplicates at 37ºC 5%CO_2. A fraction of volume of migrated cells was collected and counted using Fluorophore counting beads (Beckman Coulter). Expression of CD45, CD19 and CD5 was analyzed by flow cytometry. The remaining cells were used for DNA/RNA isolation using AllPrep DNA/RNA Micro kit (QIAGEN).

Targeted DNA sequencing (Targeted-DNAseq)

DNA was isolated using AllPrep DNA/RNA Micro Kit or Mini Kit (QIAGEN) and quantified using Qubit dsDNA BR Assay Kit (Thermo Fisher Scientific). DNA was sequenced with a custom NGS panel targeting codifying regions of 190 genes commonly mutated in hematological malignancies (**Table S3**). Libraries were prepared from 100ng of genomic DNA with the KAPA HyperPlus Kit chemistry and captured with KAPA HyperChoice probes (Roche Diagnostics), following the manufacturer's recommendations. Libraries were sequenced at Centre Nacional d'Anàlisi Genomic (CNAG, Barcelona, Spain) on a NovaSeq 6000 (Illumina) instrument, with a 2X150bp paired-end standard protocol at a mean depth of coverage of 2000x, to detect variants with a variant allele frequency (VAF) down to 1%.

Data analysis was performed using the sarek pipeline version 3.0.2 from nf-co.re project using the human genome build 19 (hg19)[1,2]. The output was processed using an in-house script and new annotations were performed using ANNOVAR (Mon, 8th June of 2020)[3]. High-probability oncogenic mutations were called by eliminating sequencing and mapping errors, and by filtering out variants with a minor allele frequency > 0.01,

according to gnomAD, as well as synonymous variants. Visual analysis with Integrative Genomics Viewer was performed for all cases. Cancer cell fractions (CCF) were calculated from VAF based on purity and ploidy determined by fluorescence in-situ hybridization (FISH).

RNA sequencing (RNA-seq)

Total RNA was isolated from purified T cells, isolated with EasySep Human T Cell Isolation kit (Stem Cell) or migrating isolated B cells using AllPrep® DNA/RNA Mini or Micro Kit (Qiagen) following the manufacturer's recommendations. RNA quantification was performed with Qubit™ RNA High Sensitivity kit (Invitrogen) in a Qubit™ fluorometer (Invitrogen). RNA integrity was checked by Agilent Bioanalyzer-2100 equipment (Agilent Technologies) using Agilent RNA 6000 Pico Kit (Agilent Technologies). Library preparation and sequencing was performed at CNAG institute. For each sample, one paired-end library was prepared using the SMARTseq2 protocol[4]. Samples were run on NovaSeq 6000 (Illumina) with a read length of 2x50bp paired end. For T-cell RNA sequencing, a mean of 71.23 million of paired-reads per sample, and an average of 63.64% (ranging from 52.27 to 75.53%) of uniquely mapped reads were generated. For B-cell RNA sequencing, a mean of 43.1 million of paired-reads per sample, and an average of 81.4% (ranging from 71.59 to 87.59%) of uniquely mapped reads were generated.

RNA-seq data processing and analysis

RNA-seq reads were mapped against human reference genome (GRCh38) using STAR software version 2.7.8a[5] with ENCODE parameters. Annotated genes were quantified with RSEM version 1.3.0[6] with default parameters, using the annotation version GENCODE v38 for T-cell RNA sequencing and GENCODE v41 for B cell RNA sequencing.

Differential expression analysis was performed following the same methodology for both T- and B-cell RNA sequencing, using limma v3.54.2 R package. Counts were normalized with TMM[7] and transformed with the 'voom' function into logCPM. To account for repeated measures on the same individual before and after treatment, the limma duplicateCorrelation function was used. Each linear model was fitted with the voom-transformed counts and contrasts were extracted. For T-cell RNA sequencing, an extra CIBERSORTx purity assessment was also performed[8].

Genes were considered differentially expressed (DEG) with an adjusted p-value <0.05 and were represented in heatmaps with the pheatmap R package, using voom-

transformed counts scaled by row. A functional enrichment analysis was performed on the DEG with gprofiler2 v0.1.8[9], using Gene Ontology, KEGG and Reactome databases as reference for T-cell RNA sequencing. REVIGO software (http://revigo.irb.hr/) was used to remove redundance and visualize Gene Ontology pathways introducing GO term and P value with medium (0.7) and *Homo sapiens* (9606) settings[10]. Additionally, a gene set enrichment analysis (GSEA) was performed with the lists of pre-ranked genes by a t-statistic with the R package fgsea v1.12[11], against the Hallmarks collection from MsigDB[12].

CLL cell cultures

For suspension cultures, PBMCs were thawed and plated in 48-well plates at a concentration of $2x10^6$ cells/mL in a total volume of 0.5mL of AIM-V media supplemented with 2% human plasma and 50μM β-mercaptoethanol. After 30min of resting at 37ºC 5%CO_2, cells were treated with increasing concentration of BIA (Axon MedChem) for 48 hours. Maximum concentration of DMSO (Sigma-Aldrich) was used as a control. Cells were collected and viability was assessed by Propidium iodide (BD Biosciences)/Annexin V-APC (Invitrogen) staining. In addition, CD3, CD19 and CD5 staining was included to determine early apoptotic T cells and CLL cells.

PBMCs were co-cultured with bone marrow stromal cells (BMSC) in media supplemented with 1μg/mL CD40L (Peprotech) and 1.5μg/mL CpG ODN (Invivogen) as previously described[13]. Briefly, UE6E7T-2 BMSC were seeded at a concentration of $1.5x10^4$ cells/mL in 24-well plates and incubated for 24 hours to allow cells to adhere. PBMCs were cultured at a ratio of 100:1 ($1.5x10^6$ cells/mL). Cells were treated with increasing concentration of BIA (Axon MedChem) and ibrutinib (MedChemExpress) for 24h. Maximum concentration of DMSO (Sigma-Aldrich) was used as a control. Synergy scores were calculated by using Synergyfinder[14].

Statistical Analysis

Numerical variable comparisons across different timepoints were conducted using the Wilcoxon matched-pairs rank test.

The relationship between TMBIM6 expression and Overall Survival (OS) as well as Failure-free Survival (FFS) was assessed using the Kaplan-Meier method, and the results were reported with associated 95% confidence intervals (95% CI). Univariable and multivariable Cox proportional hazards models were employed to identify differences in survival endpoints, and the hazard ratio (HR) with a 95% CI and p-value were reported.

To determine the optimal cutoff for TMBIM6 expression, the maximum log-rank method for OS was employed. No imputation was performed for missing data.

All statistical analyses were performed using GraphPad Prism version 8.0 software and R software version 4.3.1. Results were considered statistically significant if $p < 0.05$.

REFERENCES

1. Garcia M, Juhos S, Larsson M, et al. Sarek: A portable workflow for whole-genome sequencing analysis of germline and somatic variants. *F1000Research*. 2020;9.
2. Ewels PA, Peltzer A, Fillinger S, et al. The nf-core framework for community-curated bioinformatics pipelines. *Nat Biotechnol*. 2020;38(3):276-278.
3. Wang K, Li M, Hakonarson H. ANNOVAR: functional annotation of genetic variants from high-throughput sequencing data. *Nucleic Acids Res*. 2010;38(16):e164-e164.
4. Picelli S, Faridani OR, Björklund ÅK, Winberg G, Sagasser S, Sandberg R. Full-length RNA-seq from single cells using Smart-seq2. *Nat Protoc*. 2014;9(1):171-181.
5. Dobin A, Davis CA, Schlesinger F, et al. STAR: ultrafast universal RNA-seq aligner. *Bioinformatics*. 2013;29(1):15-21.
6. Li B, Dewey CN. RSEM: accurate transcript quantification from RNA-Seq data with or without a reference genome. *BMC Bioinformatics*. 2011;12:1-16.
7. Robinson MD, Oshlack A. A scaling normalization method for differential expression analysis of RNA-seq data. *Genome Biol*. 2010;11(3):1-9.
8. Steen CB, Liu CL, Alizadeh AA, Newman AM. Profiling cell type abundance and expression in bulk tissues with CIBERSORTx. *Methods Mol Biol*. 2020;2117:135-157.
9. Kolberg L, Raudvere U, Kuzmin I, Vilo J, Peterson H. gprofiler2--an R package for gene list functional enrichment analysis and namespace conversion toolset g: Profiler. *F1000Research*. 2020;9.
10. Supek F, Bošnjak M, Škunca N, Šmuc T. REVIGO summarizes and visualizes long lists of gene ontology terms. *PLoS One*. 2011;6(7):e21800.
11. Korotkevich G, Sukhov V, Budin N, Shpak B, Artyomov MN, Sergushichev A. Fast gene set enrichment analysis. *BioRxiv*. 2016:60012.
12. Liberzon A, Birger C, Thorvaldsdóttir H, Ghandi M, Mesirov JP, Tamayo P. The molecular signatures database hallmark gene set collection. *Cell Syst*. 2015;1(6):417-425.
13. Purroy N, Abrisqueta P, Carabia J, et al. Co-culture of primary CLL cells with bone marrow mesenchymal cells, CD40 ligand and CpG ODN promotes proliferation of chemoresistant CLL cells phenotypically comparable to those proliferating in vivo. *Oncotarget*. 2015;6(10):7632.
14. Zheng S, Wang W, Aldahdooh J, et al. SynergyFinder plus: toward better interpretation and annotation of drug combination screening datasets. *Genomics, Proteomics Bioinforma*. 2022;20(3):587-596.

SUPPLEMENTAL TABLES (see Excel Supplementary files)

Table S1. Patient characteristics.

Table S2. Fluorochrome-conjugated antibodies list.

Table S3. Genes included in the NGS panel.

Table S4. CIBERSORTx purity assessment from RNA sequencing of GELLC7 samples upon T cell enrichment.

Table S5. Differential expressed genes of the RNA sequencing of purified T cells.

Table S6. Significantly enriched Gene Ontology Biological Processes, KEGG and Reactome pathways of the RNA sequencing of purified T cells.

Table S7. Significant pathways of a gene set enrichment analysis against Hallmarks from MSigDB of the RNA sequencing of purified T cells.

Table S8. Differential expressed genes and significant pathways of a gene set enrichment analysis against Hallmarks from MSigDB of the RNA sequencing of purified B cells (P-value <0.05).

Table S9. Database of matched gene expression, recurrent genetic alterations, and clinical data from 566 patients from CLL-map portal.

SUPPLEMENTAL FIGURES LEGENDS

Supplemental figure S1. Ibrutinib alteration of immune cell composition of PB of CLL patients.

(A) Stacked bar plot of the percentage of immune cells in PBMCs out of CD45+ cells from CLL patients before and during ibrutinib treatment. **(B)** Absolute lymphocyte count of ibrutinib-treated CLL patients for one year. **(C)** Absolute B cell (CD19+ cells), **(D)** T cell (CD3+ cells) and **(E)** NK cell (CD3-CD56+ cells) numbers calculated by combining the immunophenotyping and blood count data. **(F)** Percentage and absolute numbers of CD8+ and **(G)** CD4+ T cells out of CD3+ T cells of CLL patients before treatment and after ibrutinib treatment and **(H)** CD4/CD8 ratio. Wilcoxon matched paired signed rank test was performed to compare statistical differences between baseline and the subsequent timepoints. Absolute counts are represented with median and interquartile ranges. For percentages, grey lines represent the dynamics of individual patients, while the blue line represents the mean values across all patients. Red dashed line represents the mean value of age-matched HD (n=10). Graphs show mean +/- SEM. (*P<0.05; **P<0.01; ***P<0.001; ****P<0.0001). PBMCs: peripheral blood mononuclear cells. Abs.: absolute. BT: before treatment. 1-12m: 1-12 months after treatment. HD: healthy donors. SEM: standard error of the mean.

Supplemental figure S2. NK cell and monocyte subpopulations.

(A) Flow cytometry dot plot showing the gating strategy of NK cell subpopulations and graphs of the percentage of NK cells (CD3-CD56+ out of CD45+ cells) and CD56brCD16- and CD56dimCD16+ NK cell subpopulations. **(B)** Gating strategy of monocyte subpopulations and graphs of the percentage of monocytes (CD14+ out of CD45+ cells) and CD14++CD16-, CD14++CD16+ and CD14+CD16++ subpopulations. Wilcoxon matched paired signed rank test was performed to compare statistical differences between baseline and the subsequent timepoints. Grey lines represent the dynamics of individual patients, while the blue line represents the mean values across all patients. Red dashed line represents the mean value of age-matched HD (n=10). (*P<0.05; **P<0.01; ***P<0.001; ****P<0.0001). Br (bright): high expression. Dim: low expression. BT: before treatment. 1-12m: 1-12 months after treatment. HD: healthy donors.

Supplemental figure S3. T cell differentiation status subtypes.

(A) Stacked bar plot of T cell differentiation status subtypes of CD8+ T cells and **(B)** CD4+ T cells. **(C)** Flow cytometry dot plot showing the gating strategy and percentages

of T Naïve (CCR7+CD45RA+), TCM (CCR7+CD45RA-), TEM (CCR7-CD45RA-) and TEMRA (CCR7-CD45RA+) subpopulations in CD8+ T cells and **(D)** CD4+ T cells. Wilcoxon matched paired signed rank test was performed to compare statistical differences between BT and the subsequent timepoints. Grey lines represent the dynamics of individual patients, while the blue line represents the mean values across all patients. Red dashed line represents the mean value of age-matched HD (n=10). (*P<0.05; **P<0.01; ***P<0.001; ****P<0.0001). TCM: T central memory cells. TEM: T effector memory cells. TEMRA: T effector memory cells re-expressing CD45RA. BT: before treatment. 1-12m: 1-12 months after treatment. HD: healthy donors.

Supplemental figure S4. Analysis of T cell exhaustion markers.

(A) Representative dot plots of the percentage of PD-1+ CD8+ and CD4+ T cells BT and after 12 months of ibrutinib. **(B)** Representative dot plots of the percentage of CD244+ CD8+ and CD4+ T cells BT and after 12 months of ibrutinib. **(C)** Representative dot plots of the percentage of CD39+ CD8+ and CD4+ T cells BT and after 12 months of ibrutinib. **(D)** Representative dot plots of the percentage of TIGIT+ CD8+ and CD4+ T cells BT and after 12 months of ibrutinib. **(E)** Representative dot plots of the percentage of CD160+ CD8+ T cells BT and after 12 months of ibrutinib. BT: before treatment. 12m: 12 months after treatment.

Supplemental figure S5. Co-expression of exhaustion markers and Th subpopulation gating strategy.

(A) Representative dot plots and the dynamics of the percentage of PD-1+CD244+ CD8+ and **(B)** CD4+ T cells. **(C)** Representative dot plots and the dynamics of the percentage of PD-1+CD39+ CD8+ and **(D)** CD4+ T cells. **(E)** Representative dot plots and the dynamics of the percentage of PD-1+TIGIT+ CD8+ and **(F)** CD4+ T cells. **(G)** Representative dot plots and the dynamics of the percentage of PD-1+CD160+ CD8+ T cells. Grey lines represent the dynamics of individual patients, while the blue line represents the mean values across all patients. Red dashed line represents the mean value of age-matched HD (n=10). (*P<0.05; **P<0.01; ***P<0.001; ****P<0.0001). BT: before treatment. 1-12m: 1-12 months after treatment. HD: healthy donors.

Supplemental figure S6. Analysis of CD4+ T cell subpopulations.

(A) Representative dot plots of Tfh cells defined as CXCR5+CD4+ T cells. **(B)** Representative dot plots of Tregs defined as CD25+CD127lo/- CD4+ T cells. **(C)** Representative gating strategy of Th1 (CCR4-CCR6-CXCR3+), Th2 (CCR4+CCR6-CXCR3-) and Th17 (CCR4+CCR6+) subpopulations out of CD4+ T cells. **(D)**

Longitudinal analysis of the percentage of Th1, Th2 and Th17 during ibrutinib treatment. Flow cytometry analyses included BT n=21, 1m n=15, 3m n=22, 6m n=24 and 12m n=14 samples. Wilcoxon matched paired signed rank test was performed to compare statistical differences between BT and the subsequent timepoints. Grey lines represent the dynamics of individual patients, while the blue line represents the mean values across all patients. Red dashed line represents the mean value of age-matched HD (n=10). (*P<0.05; **P<0.01; ***P<0.001; ****P<0.0001). Tfh: T follicular helper. BT: before treatment. 1-12m: 1-12 months after treatment. Tregs: T regulatory cells. Th: T helper. HD: healthy donors.

Supplemental figure S7. T cell purity assessed by flow cytometry. 6m: 6 months after treatment.

Supplemental figure S8. Analysis of T cell RNAseq from ibrutinib-treat CLL patients.

(A) REVIGO plot representation of the main GO: BP significantly enriched (P-value < 0.05) from an overrepresentation analysis of the 205 DEGs. **(B)** Changes of the T cell subpopulations assessed by CIBERSORTx deconvolution from RNAseq data. REVIGO: reduce + visualize Gene Ontology. GO: Gene Ontology. BP: biological process. BT: before treatment. 6m: 6 months after treatment. RNAseq: RNA sequencing.

Supplemental figure S9. Secretion of soluble proteins of T cells after ibrutinib treatment. Effect of ibrutinib on the secretion of soluble proteins related to immune response (IL-2, IL-4, IL-6, IL-10, IL-17A, IFNγ, TNFα, Fas, FasL, granzyme B, granzyme A, perforin and granulysin) from cell supernatants of PBMCs of CLL patients detected after 3 days of unspecific TCR stimulation. Grey lines represent the dynamics of individual patients, while the blue line represents the median values across all patients. Red dashed line represents the median value of age-matched HD (n=6). (*P<0.05; **P<0.01; ***P<0.001; ****P<0.0001). PBMCs: peripheral blood mononuclear cells. TCR: T cell receptor. BT: before treatment. 6-12m: 6-12 months after treatment. HD: healthy donors.

Supplemental figure S10. Ibrutinib altered immunosuppression, adhesion, and migration proteins in CLL cells.

(A) Representative histograms and dot plots of CD200, BTLA, PD-L1 and PD-1 expressions on CLL cells during ibrutinib treatment. **(B)** Representative histogram and dot plots of CD44, CD62L and CD49d expressions on CLL cells during ibrutinib

treatment. **(C)** Representative histograms and dot plot of CXCR5, CCR7 and CXCR4 expressions on CLL cells during ibrutinib treatment. The surface markers expressed in virtually all CLL cells were represented with the MFI. BT: before treatment. 1-12m: 1-12 months after treatment. FMO: fluorescence minus one. MFI: mean fluorescence intensity.

Supplemental figure S11. Targeted DNA sequencing results for non-migrated cells CLL cells.

Representation of the changes in CCF of the subclones detected by targeted DNA sequencing between non-migrated CLL cells from BT and 6m and phylogenetic model inferred represented by Fish plots. Multiple mutations with a CCF<0.1 in a same patient were considered different subclones**.** CCF: cancer cell fraction. BT: before treatment. 6m: 6 months after treatment.

Supplemental figure S12. Prognostic value of the DEGs in cells with retained migration under BTK inhibition.

Evaluation of the prognostic value in terms of OS and FFS of the expression of DEGs in cells with retained migratory capacity under ibrutinib. Expression of *ZNF425* was not available. Cox proportional hazards models were employed to identify differences in survival endpoints, and the HR with a 95% CI and p-value were reported. To determine the optimal cutoff for the expression, the maximum log-rank method for OS was employed. OS: overall survival. FFS: failure-free survival. DEGs: differential expressed genes. HR: hazard ratio. CI: confidence interval. Ref.: reference.

Supplemental figure S13. *TMBIM6* expression as a prognostic factor in CLL.

(A) Kaplan-Meier curve of OS based on *TMBIM6* high/low expression (cut-off: 2.39). **(B)** Kaplan-Meier curve of FFS based on *TMBIM6* high/low expression (cut-off: 2.39). OS: overall survival. FFS: failure-free survival. CI: confidence interval. HR: hazard ratio. Ref.: reference. N.: number.

Supplemental figure S14. *TMBIM6* expression is a prognostic factor in CLL, regardless of *IGHV* status.

(A) Kaplan-Meier curve of OS based on *TMBIM6* high/low expression (cut-off: 2.39) and *IGHV* mut/unmut. **(B)** Kaplan-Meier curve of FFS based on *TMBIM6* high/low expression (cut-off: 2.39) and *IGHV* mutational status. OS: overall survival. FFS: failure-free survival. CI: confidence interval. HR: hazard ratio. Ref.: reference. N.: number. IGHV: immunoglobulin heavy chain variable region.

Supplemental figure S15. *TMBIM6* expression is a prognostic factor in CLL, regardless of other clinical variables. (A) Univariable and multivariable analysis of *TMBIM6* expression, clinical data, and recurrent genetic alterations in CLL. **(B)** *TMBIM6* expression in CLL patients with amp(12). **(C)** Kaplan-Meier curve of overall survival based on *TMBIM6* high/low expression and amp(12) (cut-off: 2.39). OS: overall survival. FFS: failure-free survival. CI: confidence interval. HR: hazard ratio. Ref.: reference. N.: number. IGHV: immunoglobulin heavy chain variable region.

Supplemental figure S16. Targeting *TMBIM6* in CLL using BIA.

(A) Flow cytometry dot plot of PI versus AV to assess viable (AV-PI-), and early (AV+PI-) and late (AV+PI+) apoptotic cell populations. **(B)** Relative CLL cell viability upon 48h of BIA treatment in suspension culture. **(C)** Relative T cell viability upon 48h of BIA treatment in suspension culture. **(D)** ZIP and Bliss synergy scores calculations of the synergistic effect of the combination ibrutinib plus BIA. PI: Propidium Iodide. AV: annexin-V. DMSO: Dimethyl sulfoxide. Pt.: patient. ZIP: Zero Interaction Potency.

Supplemental figure S1

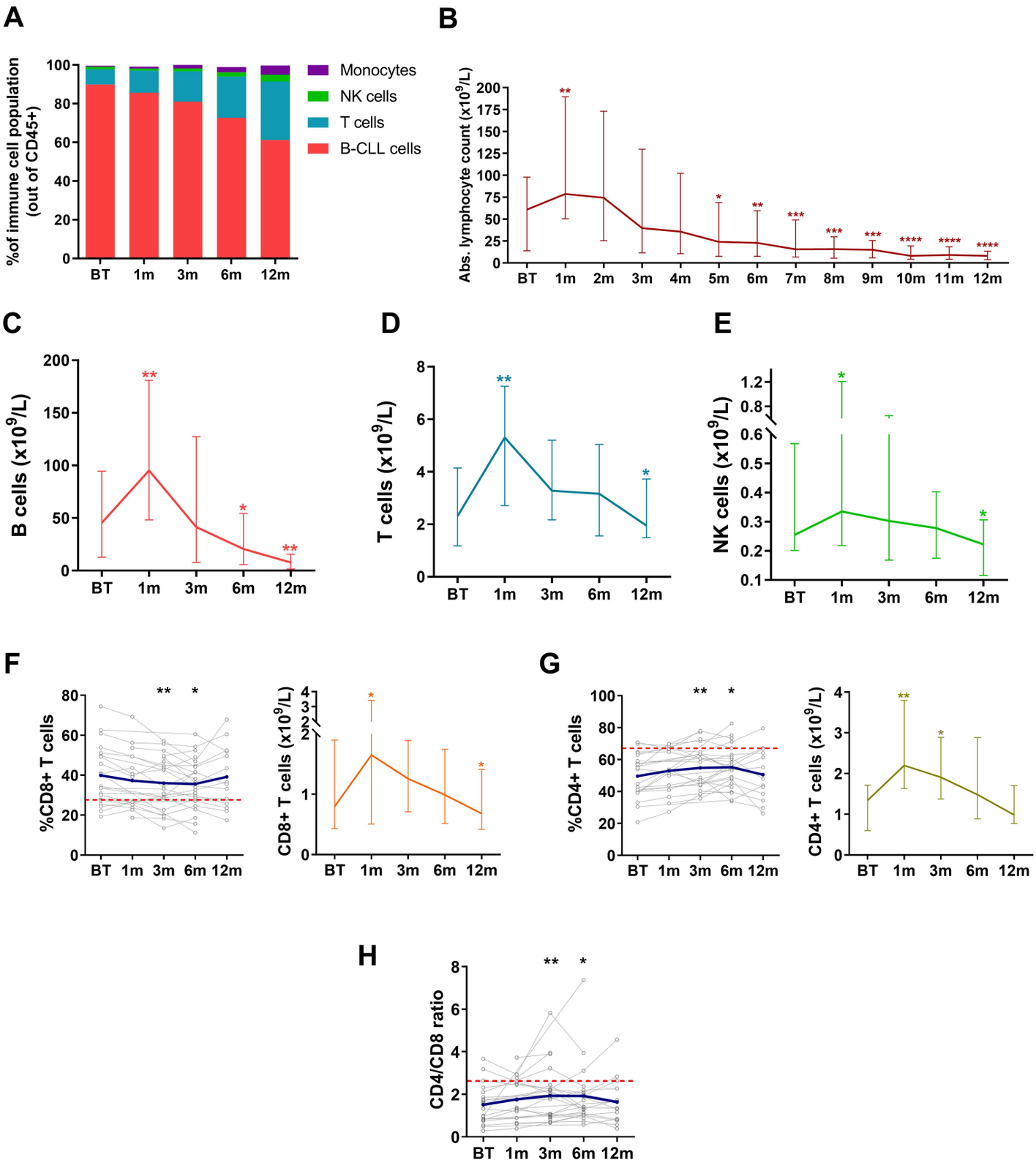

Supplemental figure S2

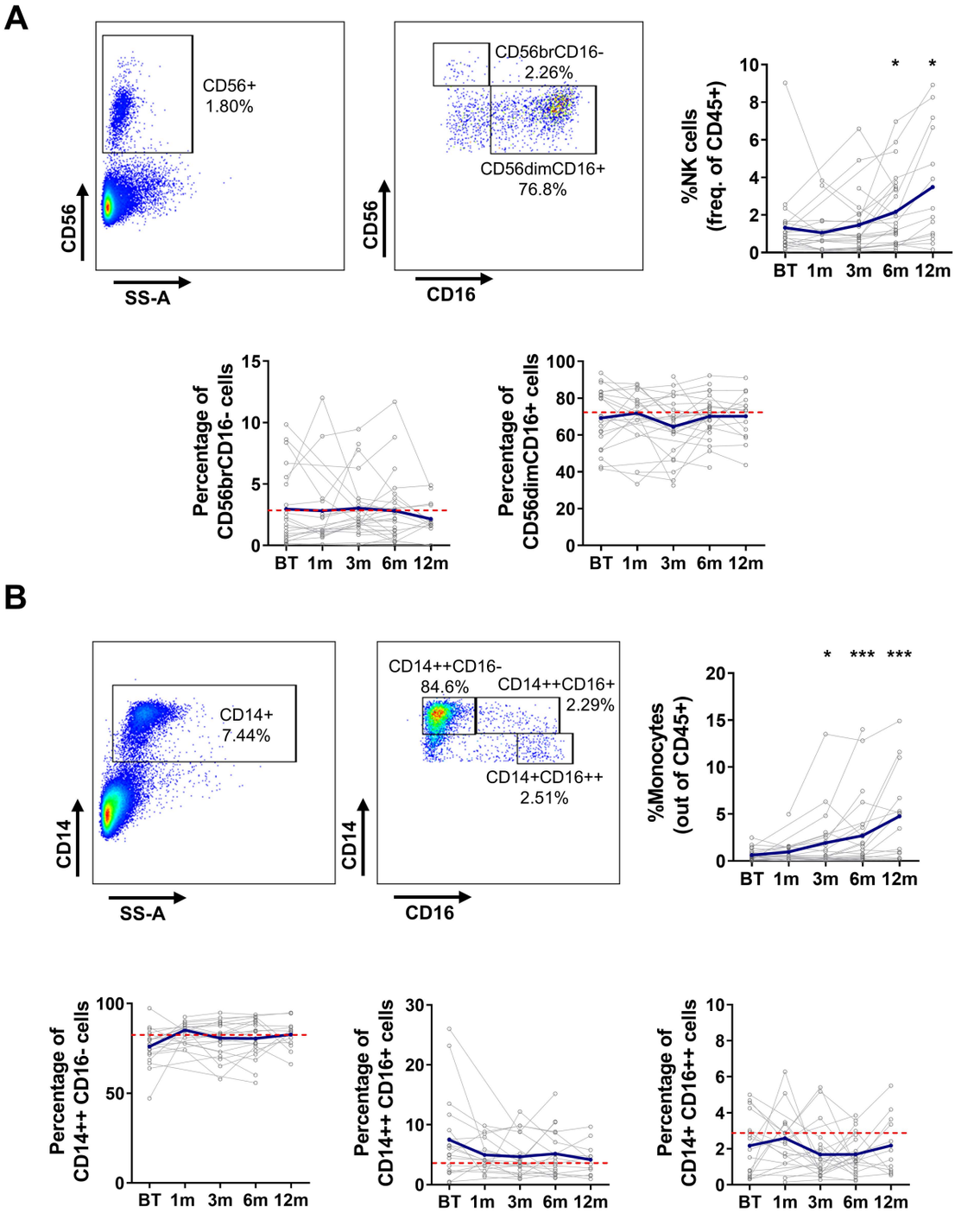

Supplemental figure S3

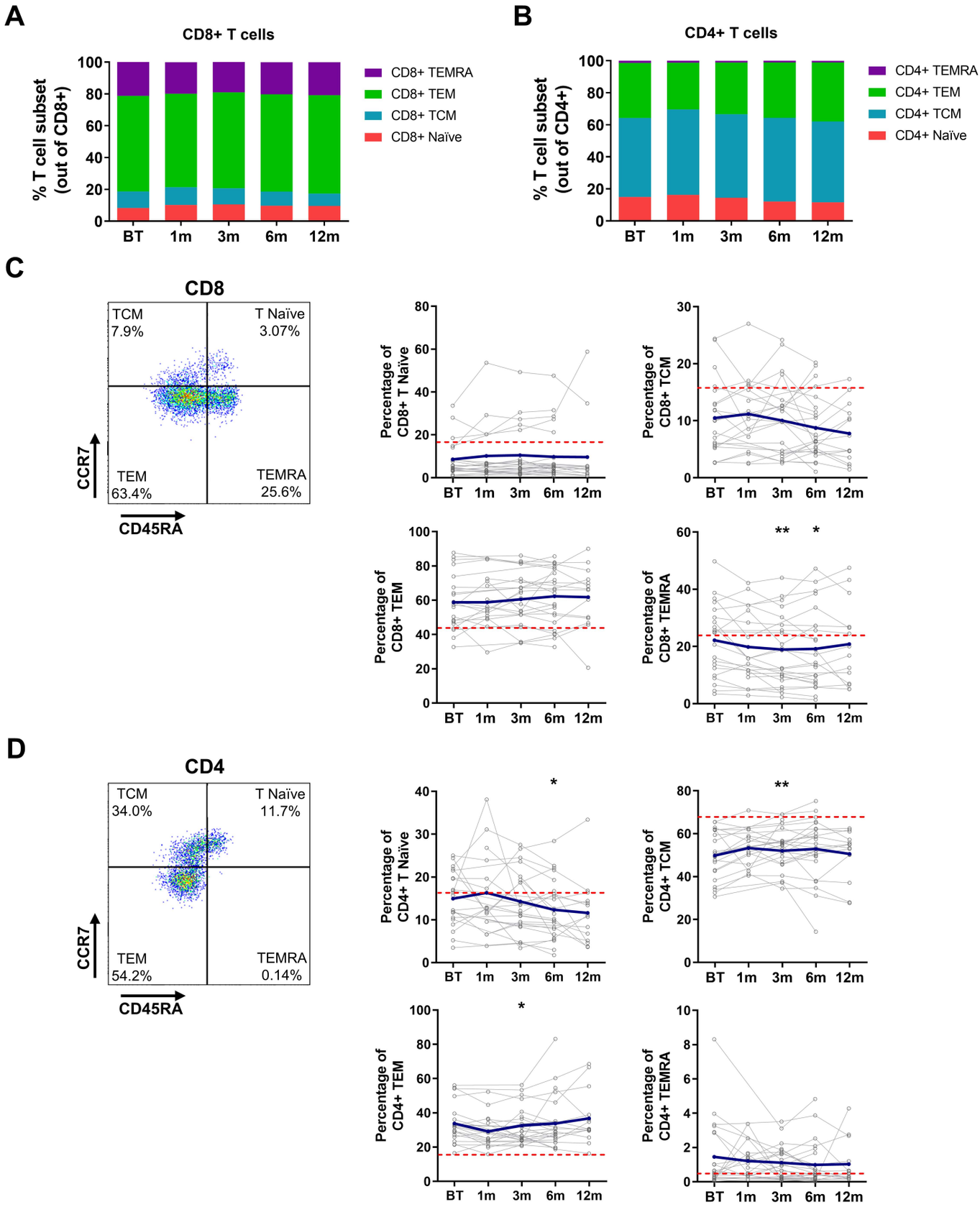

Supplemental figure S4

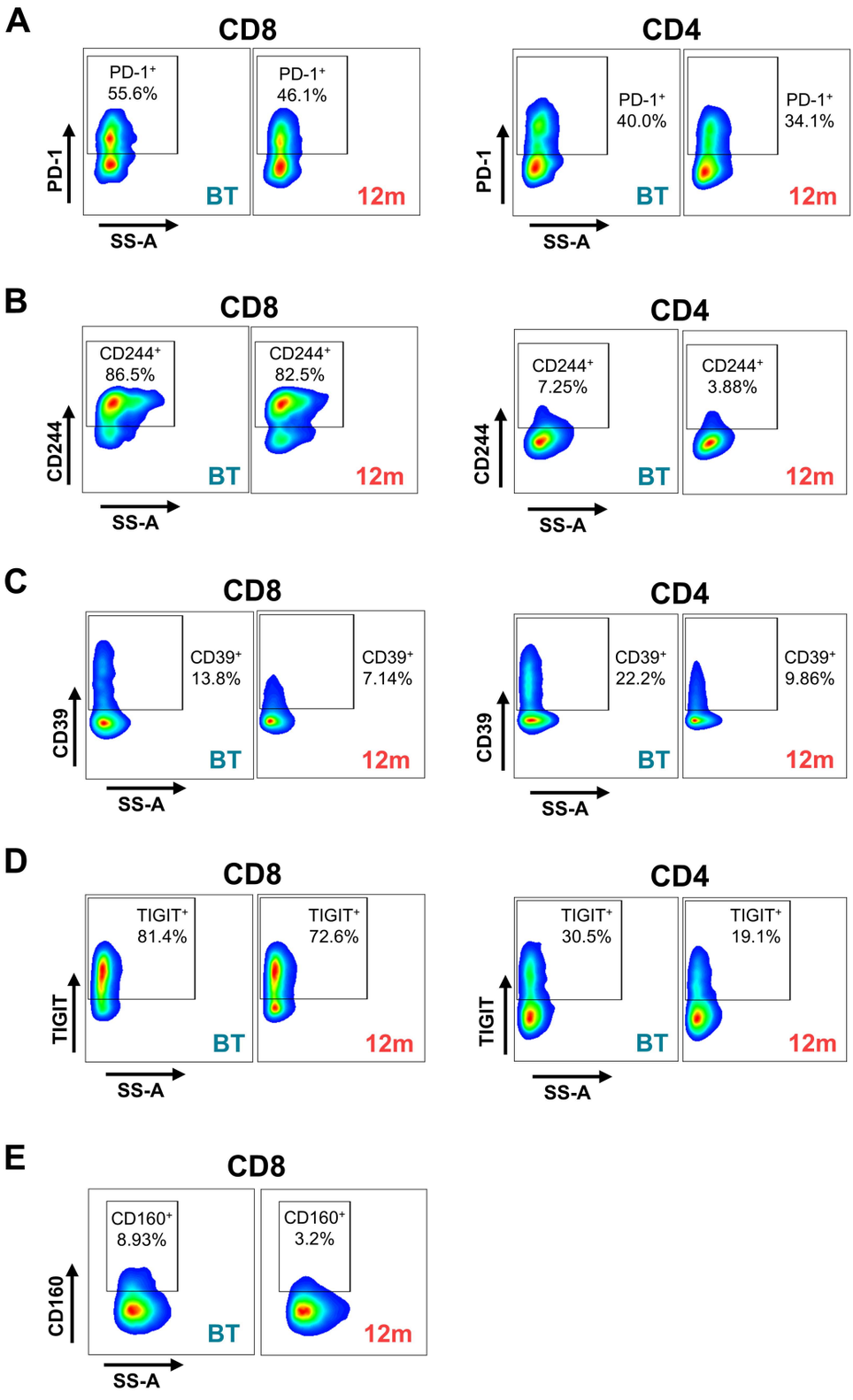

Supplemental figure S5

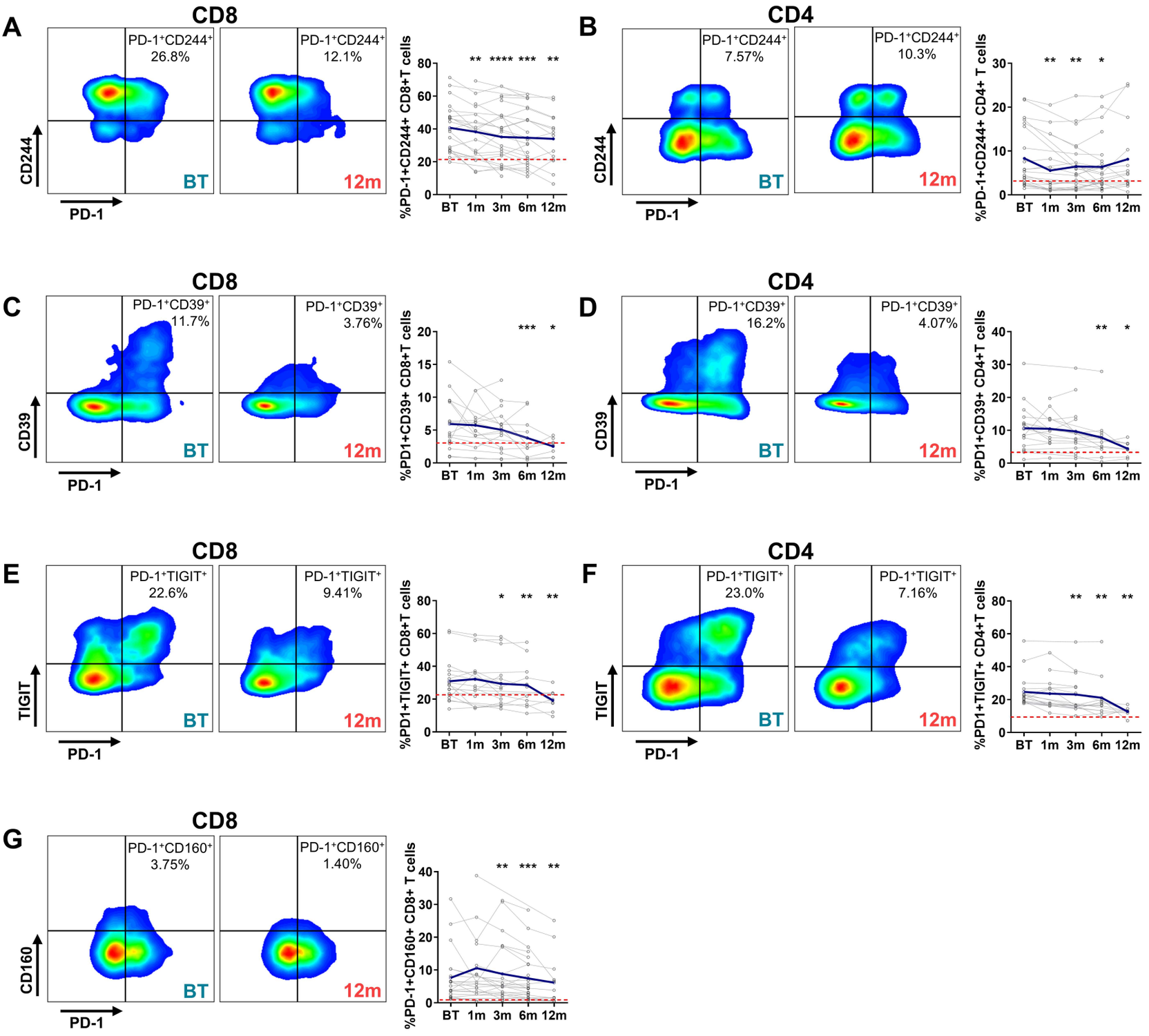

Supplemental figure S6

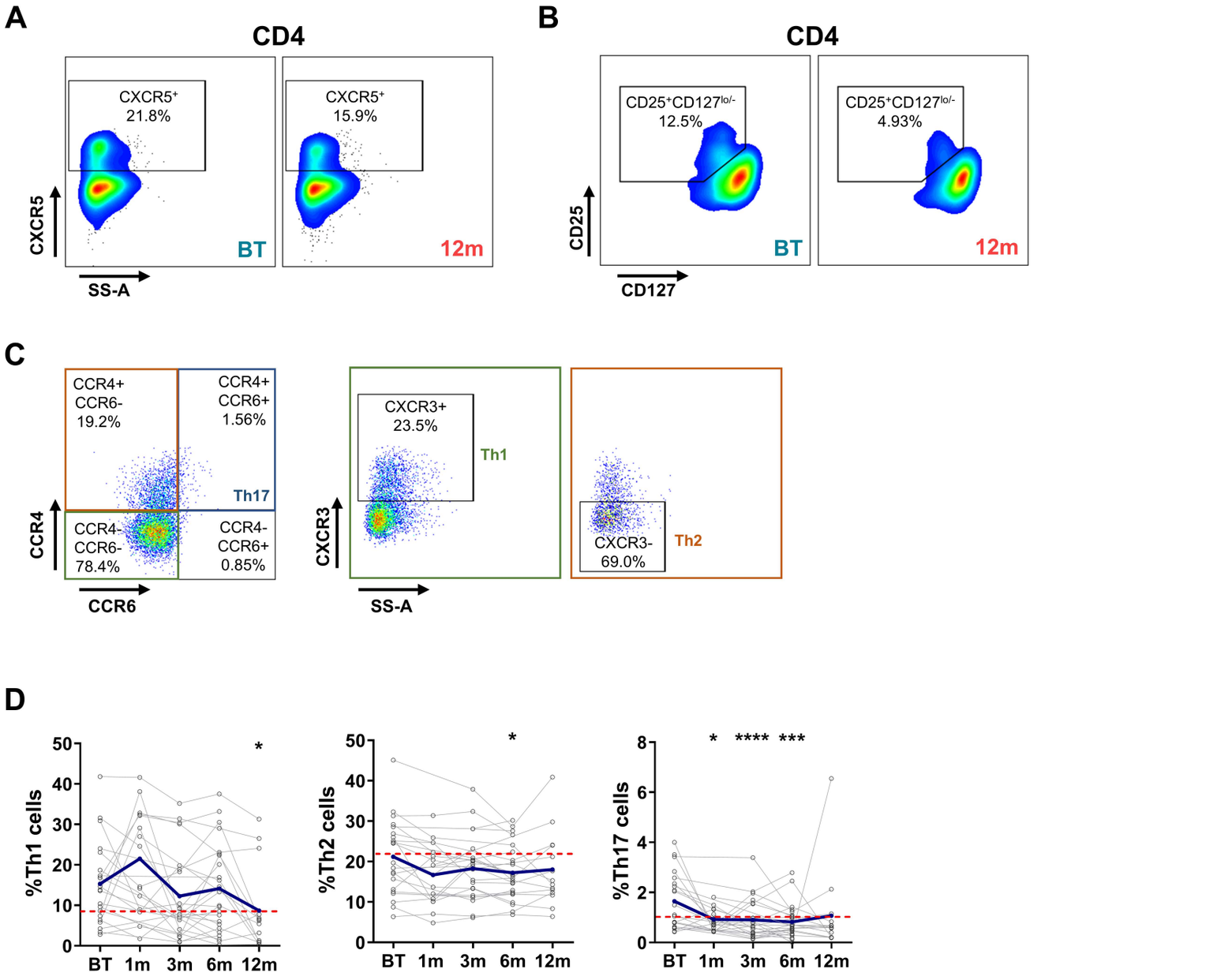

Supplemental figure S7

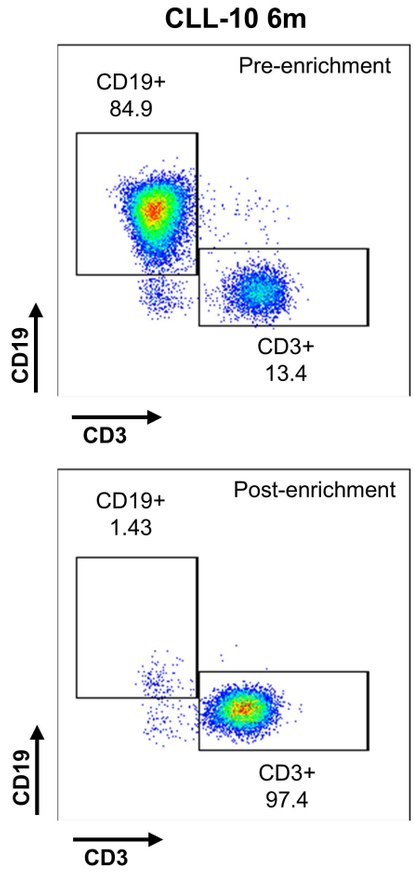

	T cell enrichment	
ID	%CD3+ cells	%CD19+ cells
CLL-01 BT	87.1	11.2
CLL-01 6m	93.3	4.52
CLL-02 BT	91.8	5.58
CLL-02 6m	91.3	2
CLL-03 BT	90.1	8.45
CLL-03 6m	98.6	0.2
CLL-04 BT	92.5	6.08
CLL-04 6m	97	0.77
CLL-05 BT	96.7	1.71
CLL-05 6m	92.9	1.03
CLL-07 BT	56	36.9
CLL-07 6m	79.4	17.2
CLL-09 BT	98.9	0.58
CLL-09 6m	99.2	0.24
CLL-10 BT	96.4	2.52
CLL-10 6m	97.4	1.43
CLL-11 BT	96.5	1.85
CLL-11 6m	90.2	8.04
CLL-12 BT	96.3	0.86
CLL-12 6m	97.3	0.86
CLL-13 BT	91	5.73
CLL-13 6m	94.4	2
Mean	**92.01**	**5.44**
Median	**93.85**	**2.00**

Supplemental figure S8

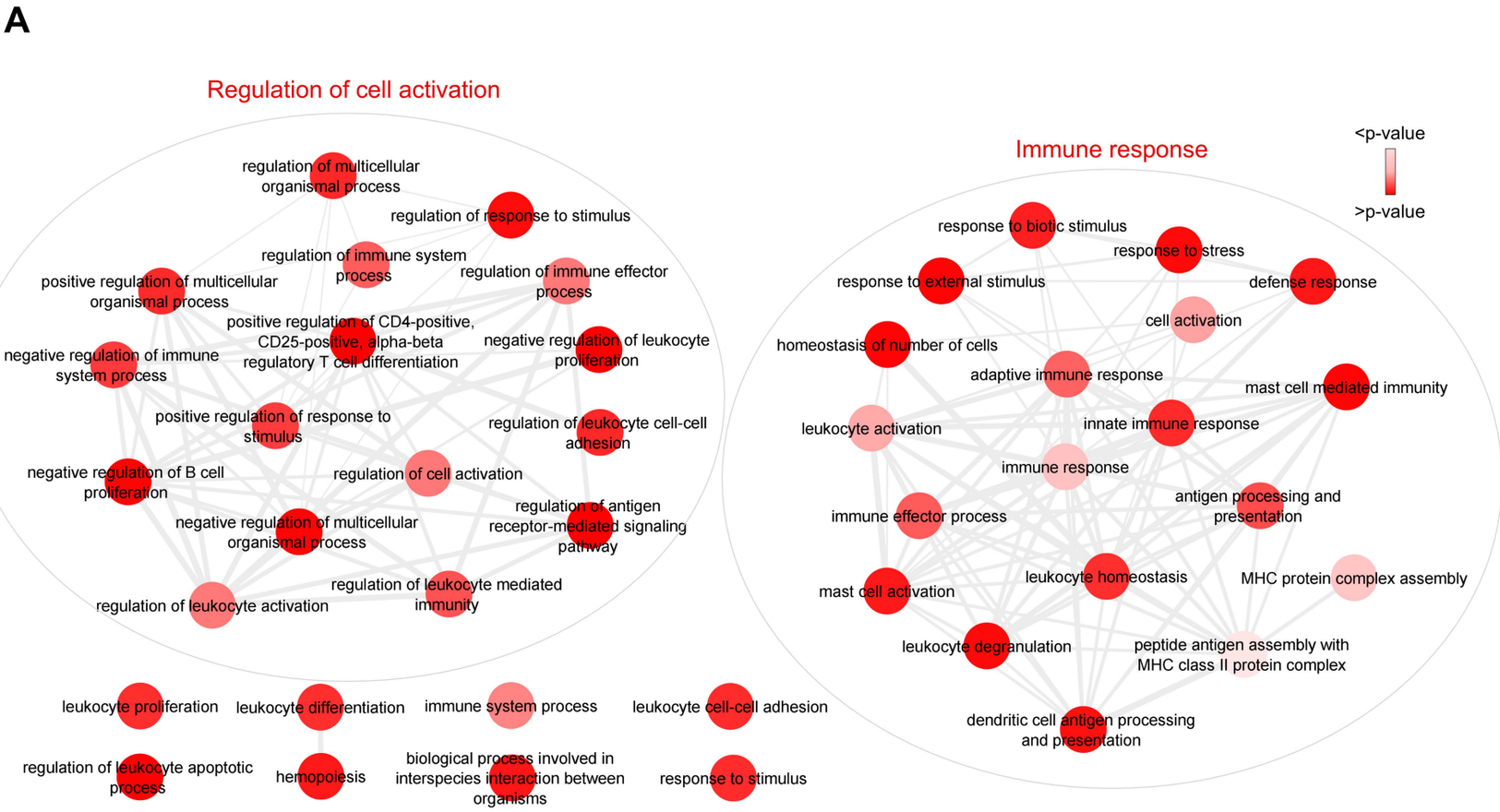

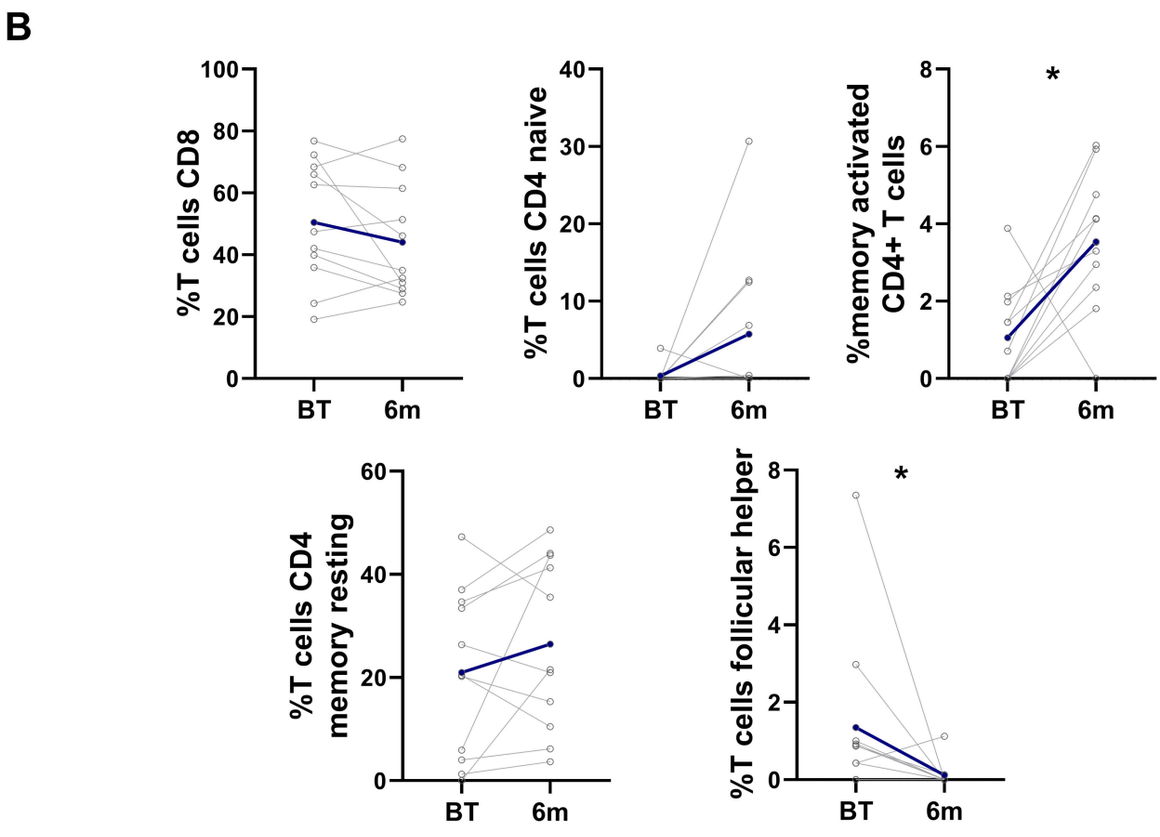

Supplemental figure S9

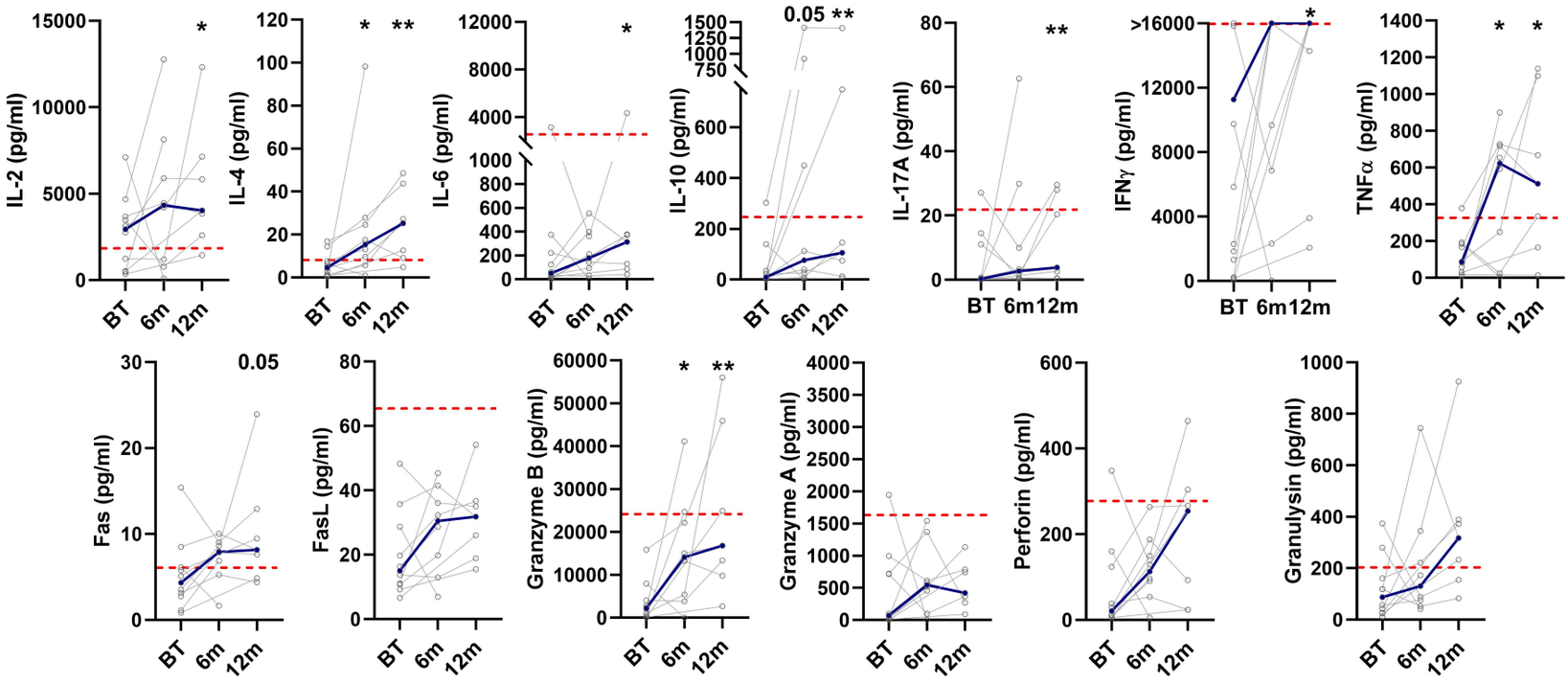

Supplemental figure S10

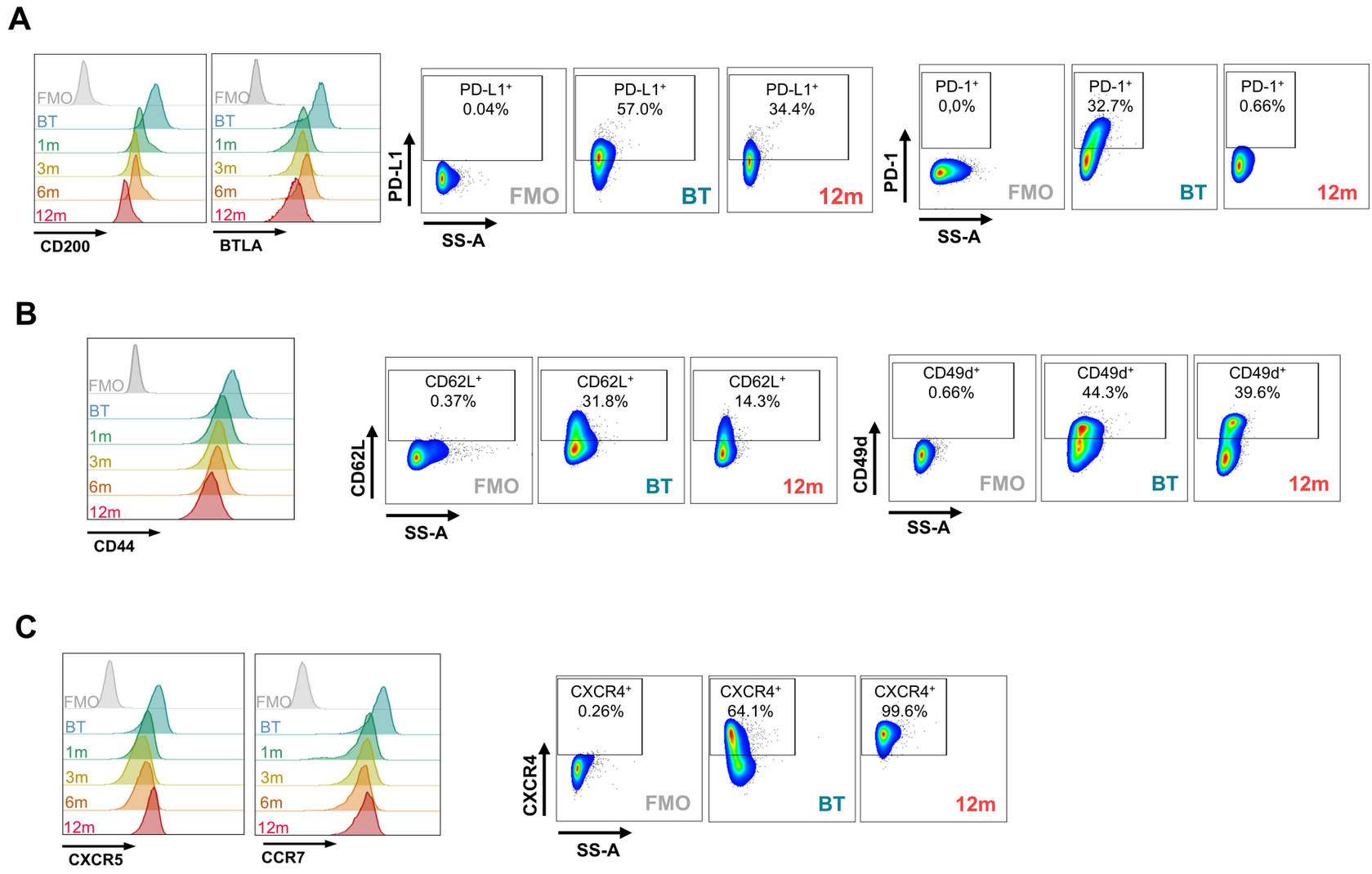

Supplemental figure S11

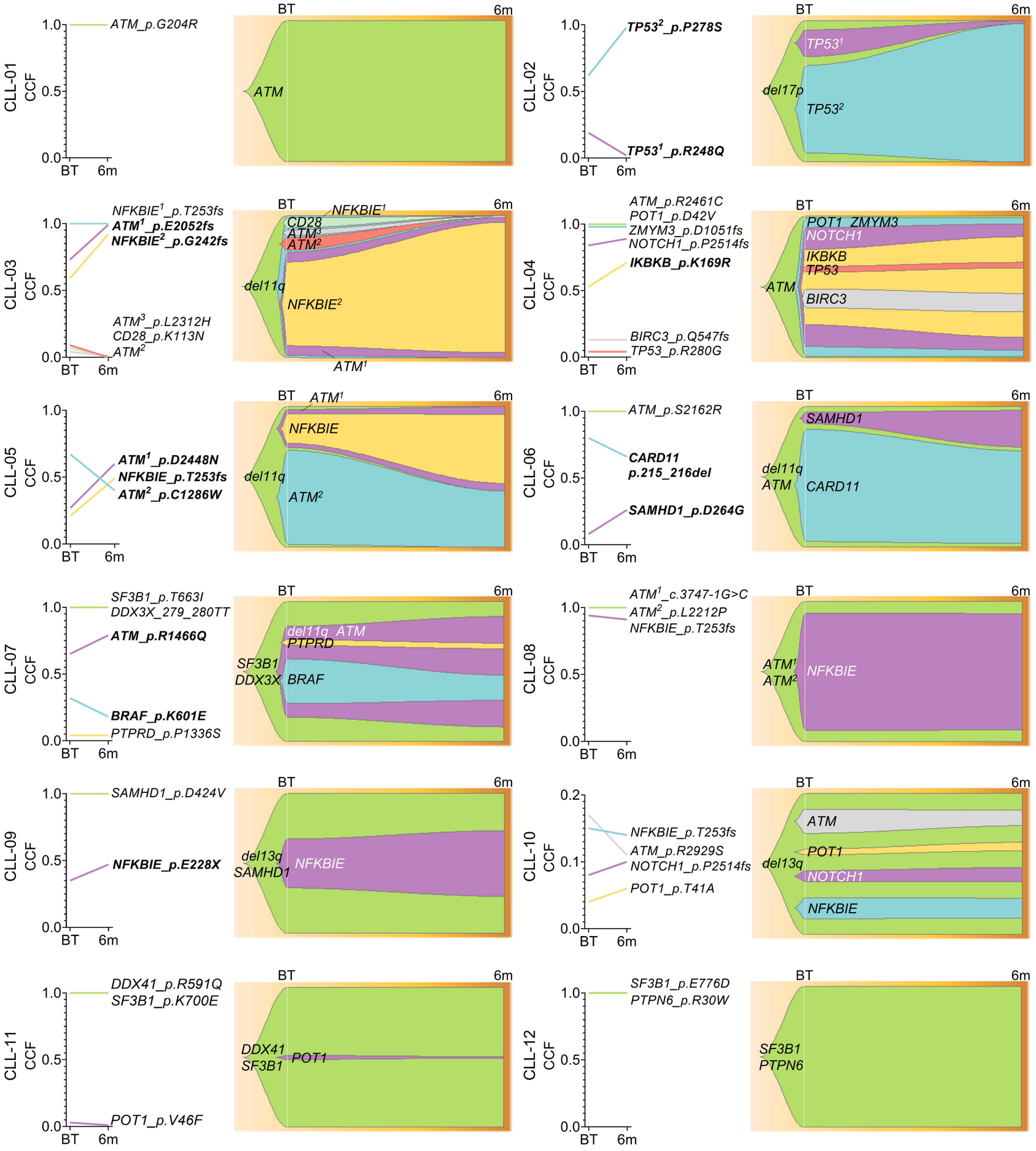

Supplemental figure S12

				OS		FFS	
	Gene	Expression	n	Hazard ratio (95% CI)	p-value	Hazard ratio (95% CI)	p-value
UPREGULATED GENES	*TMBIM6*	≤2.39	481	Ref.	–	Ref.	–
		>2.39	85	2.23 (1.56 - 3.18)	<0.001	1.51 (1.15 - 1.98)	<0.001
	CD63	≤1.78	373	Ref.	–	Ref.	–
		>1.78	193	1.99 (1.47 - 2.7)	<0.001	1.4 (1.13 - 1.73)	<0.001
	MT-CO1	≤4.33	418	Ref.	–	Ref.	–
		>4.33	148	1.33 (0.97 - 1.83)	0.08	1.33 (1.06 - 1.67)	0.01
	B2M	≤3.42	180	Ref.	–	Ref.	–
		>3.42	386	1.19 (0.85 - 1.67)	0.31	0.86 (0.69 - 1.08)	0.19
DOWNREGULATED GENES	*HLA-DMA*	≤3.01	479	Ref.	–	Ref.	–
		>3.01	87	1.61 (1.12 - 2.31)	0.01	1.39 (1.06 - 1.81)	0.02
	GGA2	≤2.56	327	Ref.	–	Ref.	–
		>2.56	239	1.47 (1.09 - 1.98)	0.01	1.18 (0.96 - 1.45)	0.12
	IRF8	≤2.71	437	Ref.	–	Ref.	–
		>2.71	129	1.46 (1.05 - 2.05)	0.03	1.58 (1.25 - 1.99)	<0.001
	EZR	≤3.07	481	Ref.	–	Ref.	–
		>3.07	85	1.46 (1 - 2.13)	0.05	1.46 (1.11 - 1.91)	0.01
	RUBCNL	≤2.41	236	Ref.	–	Ref.	–
		>2.41	330	1.5 (1.08 - 2.07)	0.01	1.26 (1.02 - 1.56)	0.04
	PIM2	≤2.37	281	Ref.	–	Ref.	–
		>2.37	285	1.24 (0.91 - 1.68)	0.17	1.11	0.32
	TSC22D3	≤3.12	467	Ref.	–	Ref.	–
		>3.12	99	0.7 (0.45 - 1.08)	0.11	0.98 (0.74 - 1.29)	0.87
	CNBP	≤2.67	224	Ref.	–	Ref.	–
		>2.67	342	0.68 (0.5 - 0.92)	0.01	0.87 (0.7 - 1.07)	0.18
	ARHGAP25	≤2.15	122	Ref.	–	Ref.	–
		>2.15	444	0.57 (0.41 - 0.79)	<0.001	0.69 (0.54 - 0.88)	<0.001
	IL10RA	≤2.39	104	Ref.	–	Ref.	–
		>2.39	462	0.51 (0.36 - 0.72)	<0.001	0.69 (0.53 - 0.89)	<0.001

Supplemental figure S13

A

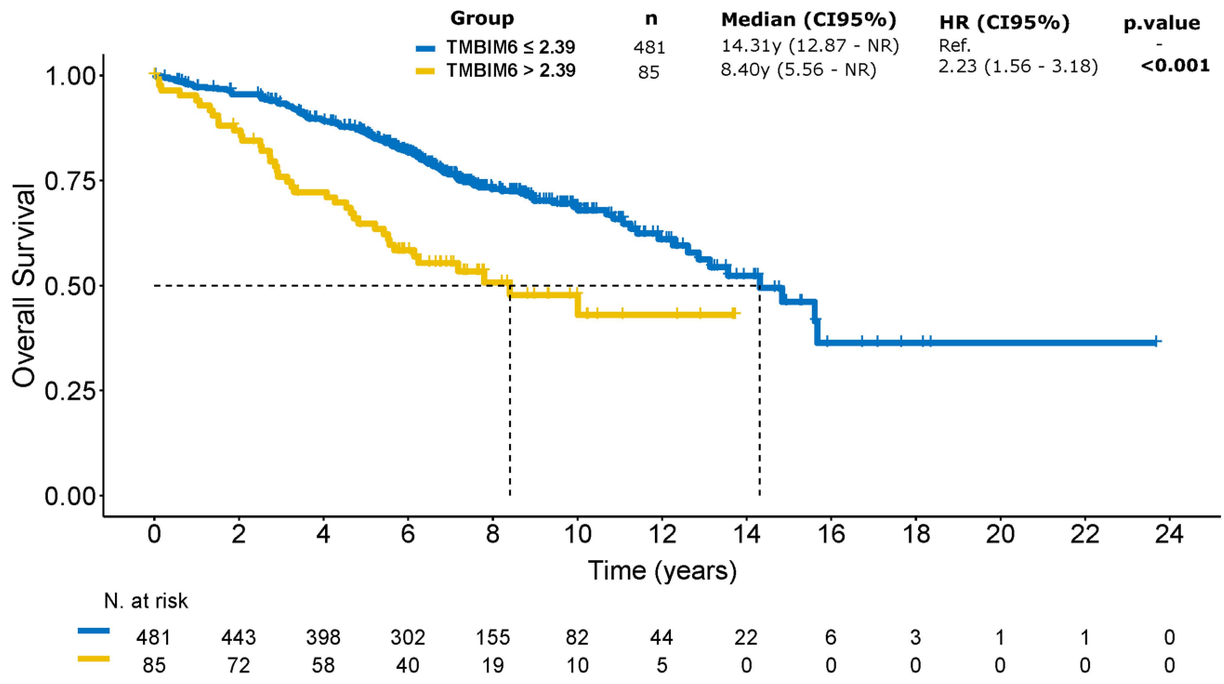

B

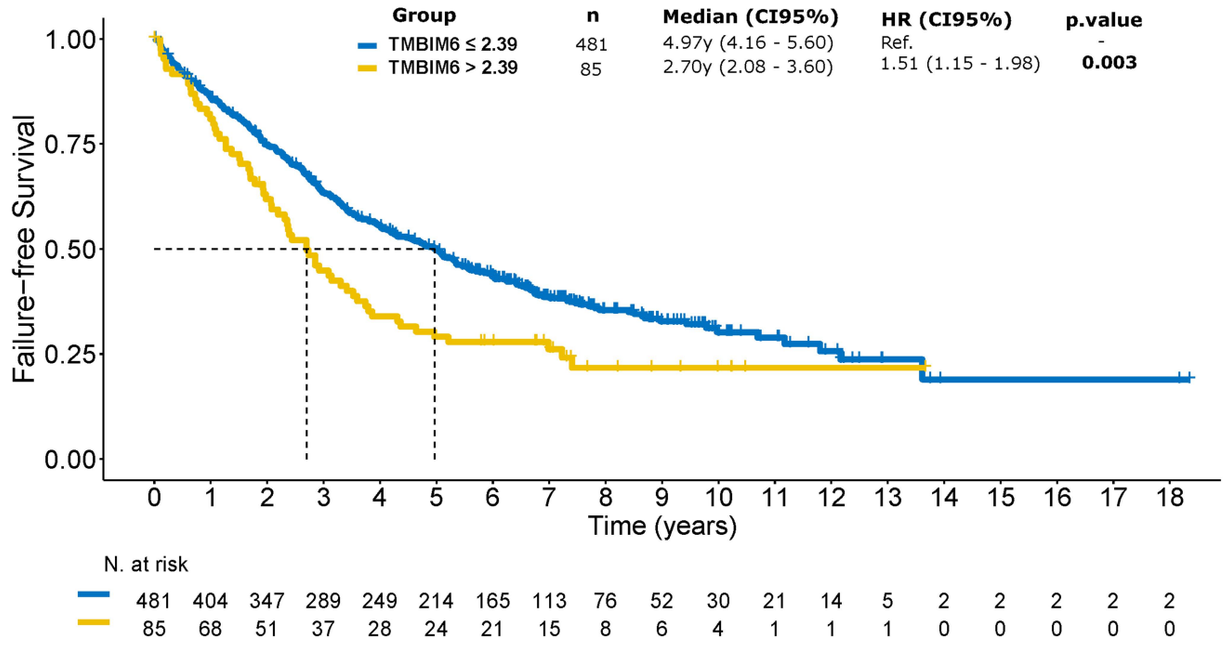

Supplemental figure S14

A

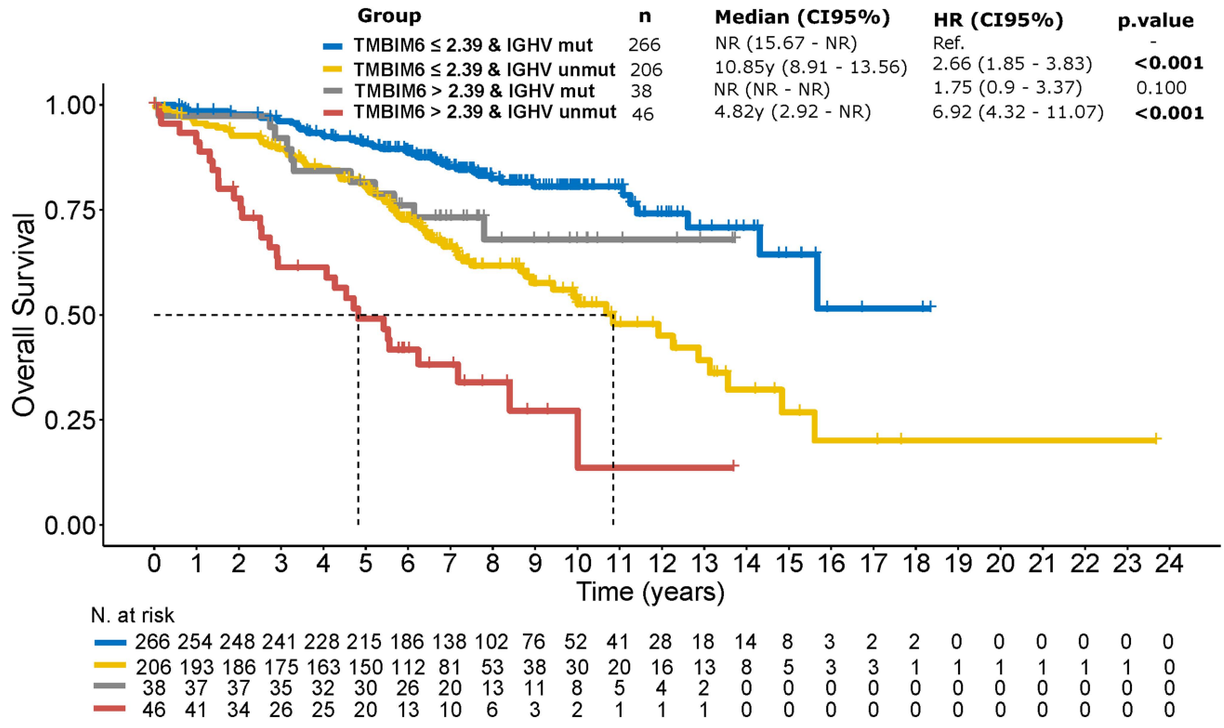

B

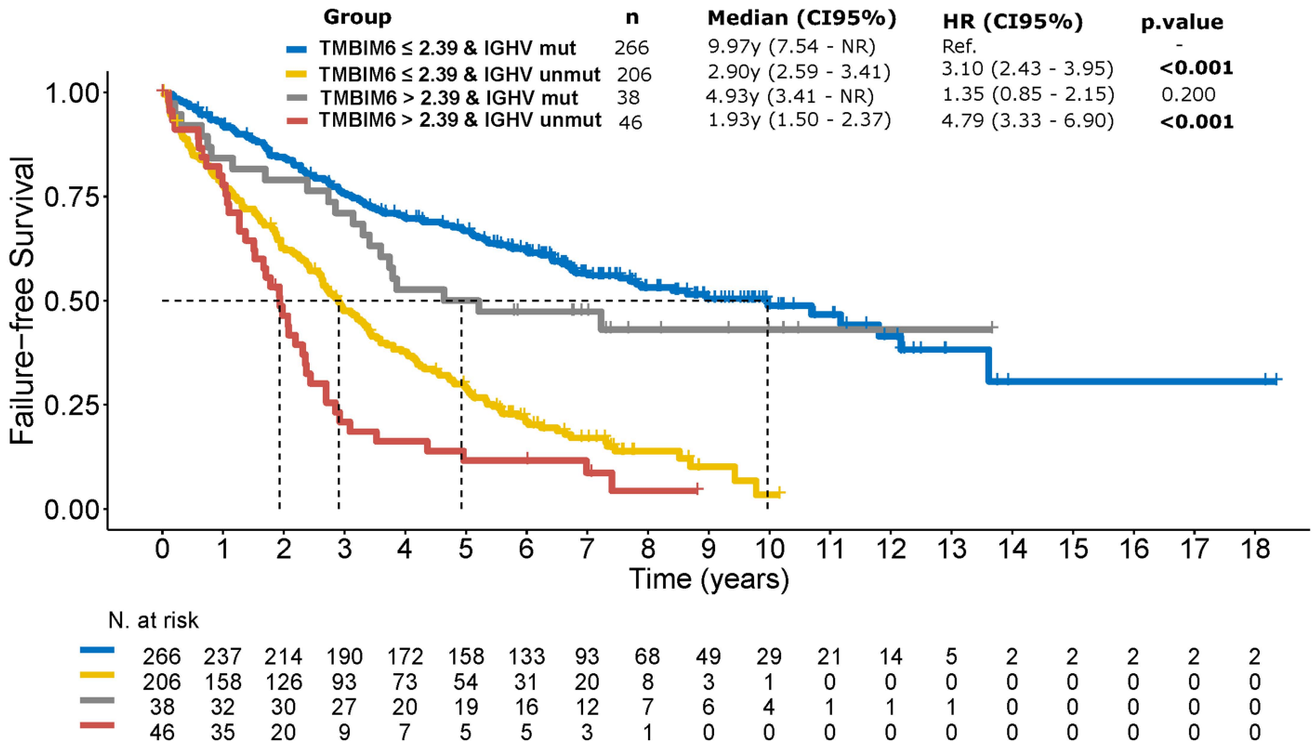

Supplemental figure S15

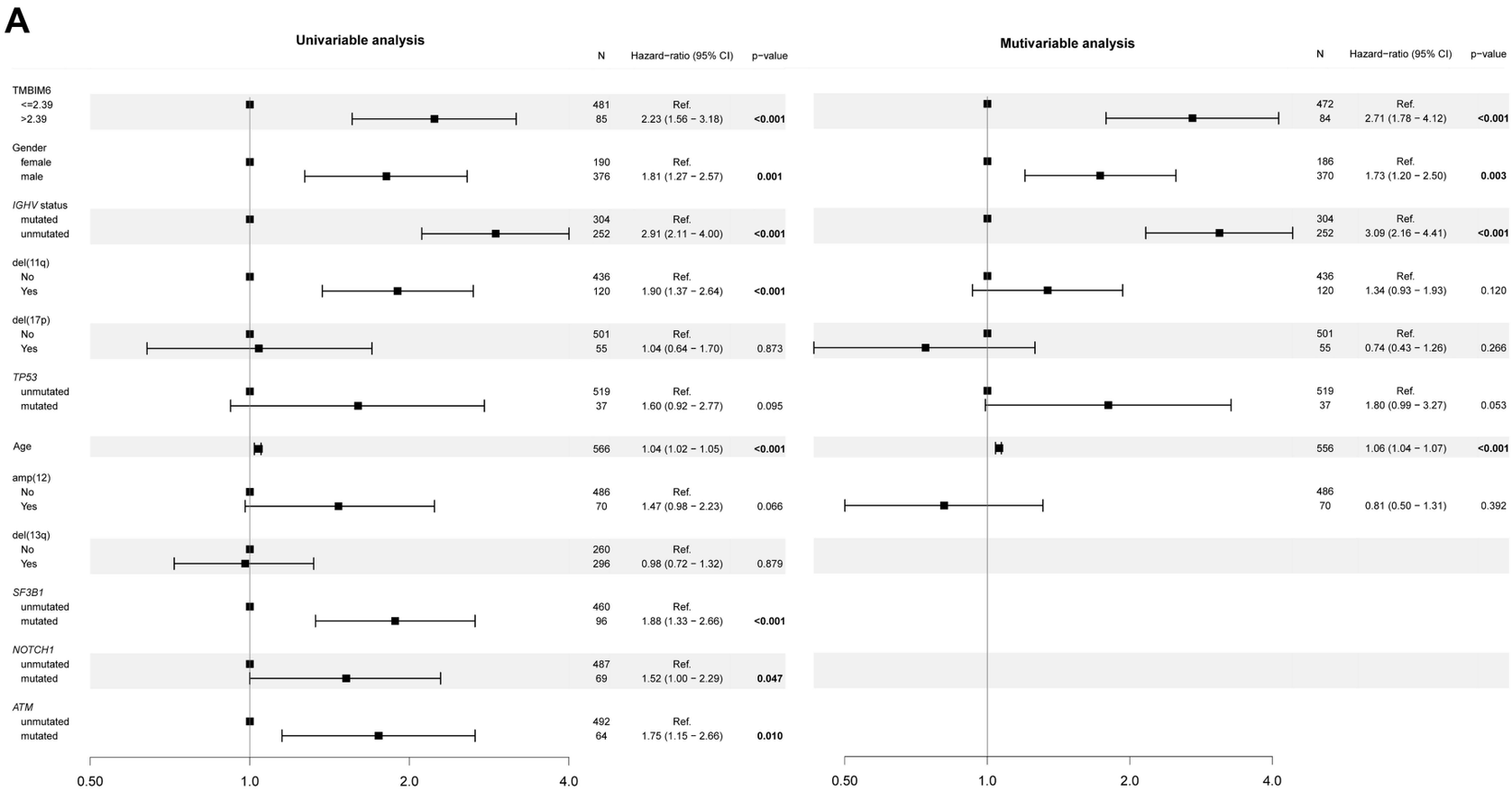

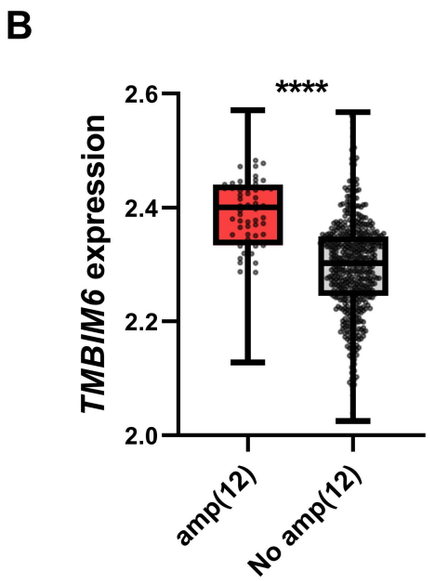

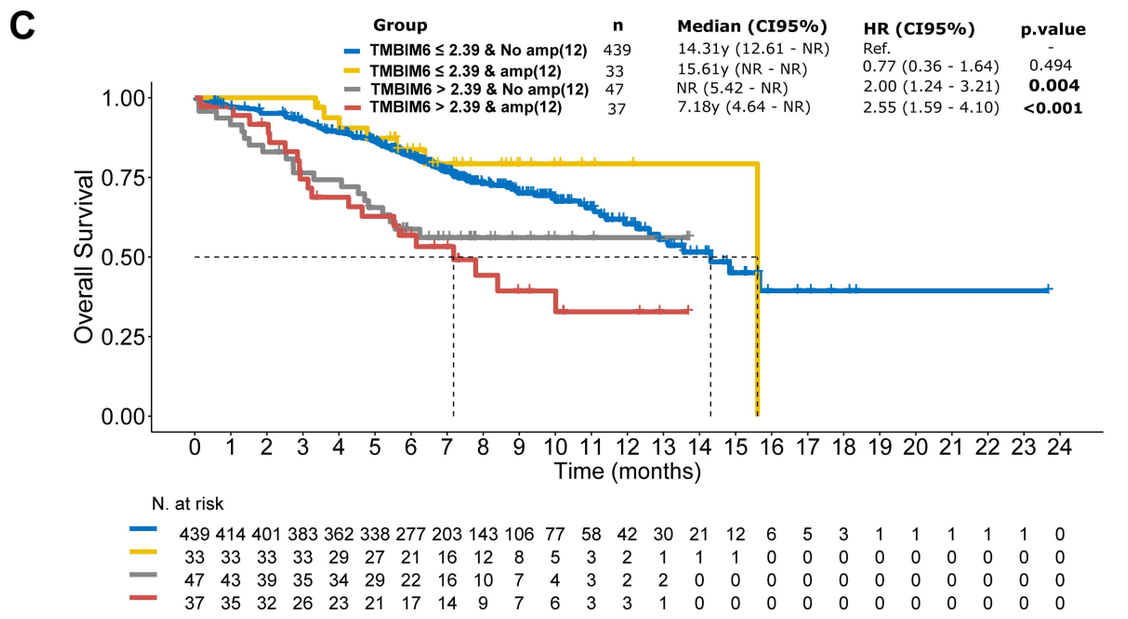

Supplemental figure S16